Wind and Structures, Vol. 2, No. 4 (1999) 267-284
DOI: http://dx.doi.org/10.12989/was.1999.2.4.267

Multiple tuned mass dampers for controlling coupled buffeting and flutter of long-span bridges

Yuh-Yi Lin†, Chii-Ming Cheng‡ and Chung-Hau Lee‡†

Department of Civil Engineering, Tamkang University, Tamsui, Taiwan 251, R.O.C.

Abstract. Multiple tuned mass dampers are proposed to suppress the vertical and torsional buffeting and to increase the aerodynamic stability of long-span bridges. Each damper has vertical and torsional frequencies, which are tuned to the corresponding frequencies of the structural modes to suppress the resonant effects. These proposed dampers maintain the advantages of traditional multiple mass dampers, but have the added capability of simultaneously controlling vertical and torsional buffeting responses. The aerodynamic coupling is incorporated into the formulations, allowing this model to effectively increase the critical speed of a bridge for either single-degree-of-freedom flutter or coupled flutter. The reduction of dynamic response and the increase of the critical speed through the attachment of the proposed dampers to the bridge are also discussed. Through a parametric analysis, the characteristics of the multiple tuned mass dampers are studied and the design parameters - including mass, damping, frequency bandwidth, and total number of dampers - are proposed. The results indicate that the proposed dampers effectively suppress the vertical and the torsional buffeting and increase the structural stability. Moreover, these tuned mass dampers, designed within the recommended parameters, are not only more effective but also more robust than a single TMD against wind-induced vibration.

Key words: multiple tuned mass dampers; buffeting; flutter; long-span bridge.

1. Introduction

Tuned mass dampers (TMDs) have been used in many structures to control wind-induced vibrations. For long-span bridges, the aerodynamic response becomes even more significant due to their large flexibilities. The effectiveness of the TMD used in a long-span bridge has been demonstrated in analyses and experiments (Huffmann *et al.* 1987, Malhortra and Wieland 1987, Nobuto *et al.* 1988, Honda *et al.* 1993, Gu *et al.* 1998). However, the error of estimating the bridge's natural frequency or damping is inevitable in practice and this error may reduce the effectiveness of the damper. Furthermore, the massive size of the damper may cause difficulties with bridge construction and maintenance. To decrease the disadvantages of the TMD, the multiple tuned mass dampers (MTMDs) were then proposed by Xu and Igusa (1992) and Igusa and Xu (1994). Performance of the MTMDs was also extensively discussed by Yamaguchi and

† Associate Professor
‡ Professor
‡† Graduated Student

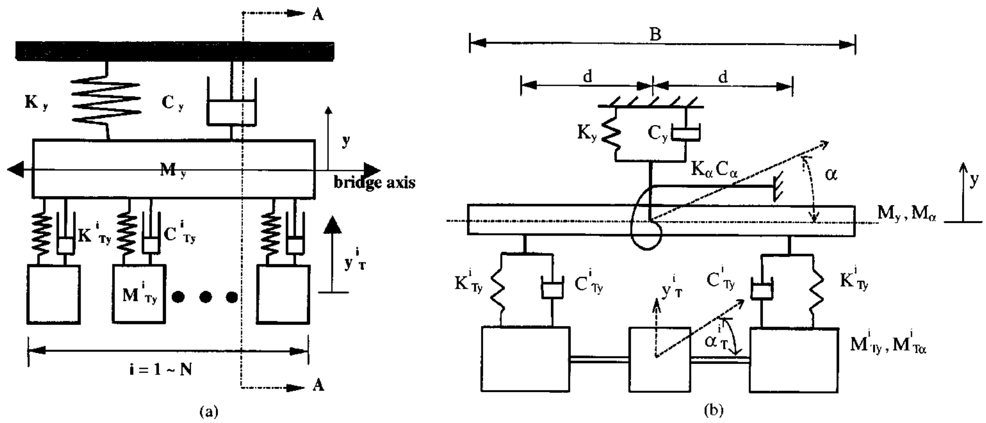

Fig. 1 Bridge - MTMDs system (a) arrangements of bridge and MTMDs (b) schematic diagram of ith TMD and bridge(section A-A of (a))

Harnpornchai (1993), Abe and Fujino (1994), Abe and Igusa (1995), Kareem and Kline (1995) and Jangrid and Datta (1997). Sun (1997) also examined the performance of the MTMDs in the long-span bridges for suppressing the buffeting response. From these studies, it can be concluded that the MTMDs are more effective and more robust than a single TMD, and the size of each TMD can be decreased to fit the primary structure.

Of the aerodynamic problems of long-span bridges, the primary concerns of bridge engineers are the vertical and torsional buffeting responses, and flutter. Huffmann *et al.* (1987) and Malhortra and Wieland (1987) used separate bending and torsional dampers to respectively reduce the flexural and torsional responses and to increase the critical speed of a cable-stayed bridge. A TMD with vertical and torsional frequencies, having the capability of reducing the vertical and torsional responses and increasing stability, was proposed by Lin *et al.* (1999). This concept is extended to the MTMDs in this paper. In this model the dampers are positioned along the bridge axis at the location where maximum response occurred (Fig. 1). Each damper is supported by two identical springs and has the vertical and torsional frequencies, which are tuned around the natural frequencies of the bridge's first vertical and first torsional modes. Since the spans of modern bridges have become longer and the decks more slender, the bridge's response and stability due to wind loads may be significantly influenced by the aerodynamic coupling. This coupling, mainly contributed by the involvement of the first vertical and first torsional modes of the bridge, is then taken into account in the formulations of the MTMD-bridge system. Therefore, the proposed model can estimate the critical velocity of the bridge for either single-degree-of-freedom flutter or coupled flutter.

In this paper an analytical model is presented to examine the performance of the proposed MTMDs used in the long-span bridge. The dynamic response reduction and the increase of the critical velocity of the flexible bridge are discussed through a parametric study. A cable-stayed bridge subjected to wind loads is chosen as the target for evaluating the performance of the MTMDs in this analysis. The effects of the design parameters such as total mass, damping, frequency range and total number of dampers on the response are studied, the values of these design parameters are suggested.

2. Formulations

The vertical or torsional motion of the long-span bridge is generally dominated by the primary structure's fundamental mode in that direction. Hence, it is feasible to model the bridge as a 2-DOF system. Each damper of the MTMDs is also modeled as a 2-DOF system. Provided that there are N dampers used in the structure, the bridge-MTMDs system, shown in Fig. 1, oscillates with 2N +2 DOF. The equations of motion of the interactions between the bridge and the MTMDs can be expressed in the generalized coordinate system as

$$M_y \ddot{y} + C_y \dot{y} + K_y y - 2\sum_{i=1}^{N} C_{Ty}^i (\dot{y}_T^i - \dot{y}) - 2\sum_{i=1}^{N} K_{Ty}^i (y_T^i - y) = \mathbf{\Phi}_y^T \mathbf{L}_f + \mathbf{\Phi}_y^T \mathbf{L}_b \tag{1}$$

$$M_{Ty}^i \ddot{y}_T^i + 2C_{Ty}^i (\dot{y}_T^i - \dot{y}) + 2K_{Ty}^i (y_T^i - y) = 0 \quad (i = 1, \mathrm{N}) \tag{2}$$

$$M_{T\alpha}^i \ddot{\alpha}_T^i + 2C_{T\alpha}^i (\dot{\alpha}_T^i - \dot{\alpha}) d^2 + 2K_{T\alpha}^i (\alpha_T^i - \alpha) d^2 = 0 \quad (i = 1, \mathrm{N}) \tag{3}$$

$$M_\alpha \ddot{\alpha} + C_\alpha \dot{\alpha} + K_\alpha \alpha - 2\sum_{i=1}^{N} C_{T\alpha}^i (\dot{\alpha}_T^i - \dot{\alpha}) d^2 - 2\sum_{i=1}^{N} K_{T\alpha}^i (\alpha_T^i - \alpha) d^2 = \mathbf{\Phi}_\alpha^T \mathbf{Mo}_f + \mathbf{\Phi}_\alpha^T \mathbf{Mo}_b \tag{4}$$

where y, α are the generalized vertical and torsional displacements, respectively; M, C and K are the generalized mass, damping and stiffness, respectively; the subscripts y, α indicate the vertical and the torsional directions of the bridge, the subscript T represents the TMD; the subscripts Ty and $T\alpha$ stand for the vertical and the torsional directions of the TMD, respectively; the superscript i designates the ith damper; $\mathbf{\Phi}$ is the matrix containing the first vertical or torsional mode of the bridge; d is the distance from vertical spring to the center of TMD; **L**, **Mo** are the lift force and pitching moment acting on the deck, respectively; the subscripts f, b designate the self-excited and buffeting forces, respectively.

The self-excited forces acting on deck node j in vertical direction L_{fj} and in torsion direction Mo_{fj} can be expressed in the following forms (Scanlan and Tomko 1971):

$$L_{fj}(t) = \frac{1}{2}\rho U^2 (2B)(K)\left[H_1^*(K)\frac{\dot{v}_j(t)}{U} + H_2^*(K)\frac{B\dot{\beta}_j(t)}{U} + KH_3^*(K)\beta_j(t) \right]\Delta L_j \tag{5}$$

$$Mo_{fj}(t) = \frac{1}{2}\rho U^2 (2B^2)(K)\left[A_1^*(K)\frac{\dot{v}_j(t)}{U} + A_2^*(K)\frac{B\dot{\beta}_j(t)}{U} + KA_3^*(K)\beta_j(t) \right]\Delta L_j \tag{6}$$

where ρ is air density; U is wind velocity; B is deck width; $K = \{(B\omega)/U\}$ is the reduced frequency; ΔL_j is the tributary length of the node j (Fig. 2); v_j, β_j are the vertical and torsional displacements at node j, respectively; H_l^*, A_l^* $(l = 1, 3)$ are the flutter derivatives.

Then, substituting Eqs. (5) and (6) into Eqs. (1)~(4) and making some manipulations, we can rewrite the equations of motion as follows:

$$\ddot{y} + (2\xi_y \omega_y - D_1\omega)\dot{y} + \omega_y^2 y + 2\sum_{i=1}^{N} (\mu_y^i \xi_{Ty}^i \omega_{Ty}^i)(\dot{y} - \dot{y}_T^i)$$
$$+ \sum_{i=1}^{N} \mu_y^i (\omega_{Ty}^i)^2 (y - y_T^i) - D_2 \omega\dot{\alpha} - E_1 \omega^2 \alpha = \mathbf{\Phi}_y^T \mathbf{L}_b / M_y \tag{7}$$

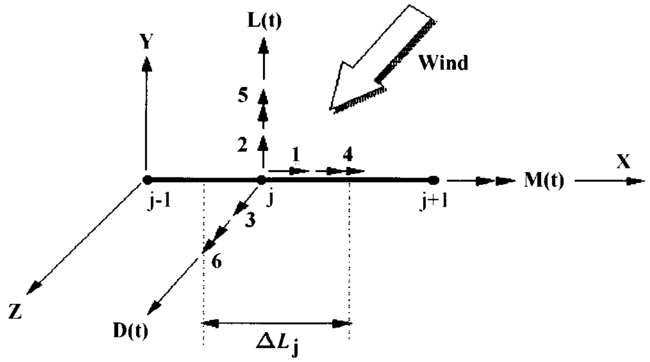

Fig. 2 Finite element model of bridge deck subjected to wind loads

$$\ddot{y}_T^i + 2\xi_{Ty}^i\,\omega_{Ty}^i\,(\dot{y}_T^i - \dot{y}) + (\omega_{Ty}^i)^2(y_T^i - y) = 0 \quad (\mathrm{i}=1,\,\mathrm{N}) \tag{8}$$

$$\ddot{\alpha}_T^i + 2\xi_{T\alpha}^i\,\omega_{T\alpha}^i(\dot{\alpha}_T^i - \dot{\alpha}) + (\omega_{T\alpha}^i)^2(\alpha_T^i - \alpha) = 0 \quad (\mathrm{i}=1,\,\mathrm{N}) \tag{9}$$

$$\ddot{\alpha} + (2\xi_\alpha\omega_\alpha - D_4\omega)\,\dot{\alpha} + (\omega_\alpha^2 - E_2\omega^2)\,\alpha + 2\sum_{i=1}^{N}\mu_\alpha^i\,\xi_{T\alpha}^i\,\omega_{T\alpha}^i(\dot{\alpha} - \dot{\alpha}_T^i)$$
$$+\sum_{i=1}^{N}\mu_\alpha^i(\omega_{T\alpha}^i)^2(\alpha - \alpha_T^i) - D_3\,\omega\dot{y} = \mathbf{\Phi}_\alpha^T\mathbf{Mo}_b/M_\alpha \tag{10}$$

where ξ_m, ω_m ($m = y$, α, Ty, $T\alpha$) are the damping ratio and circular frequency, respectively; μ_y^i, μ_α^i are the generalized mass ratio of the ith TMD to the bridge in vertical and torsional directions, respectively. The expressions of D_1-D_4 and E_1-E_2 are in the following forms:

$$D_1 = \frac{\rho}{M_y}B^2H_1^*\sum_{j=1}^{n}\phi_{yi}^2\,\Delta L_j \tag{11}$$

$$D_2 = \frac{\rho}{M_y}B^3H_2^*\sum_{j=1}^{n}\phi_{yj}\,\phi_{\alpha j}\,\Delta L_j \tag{12}$$

$$D_3 = \frac{\rho}{M_\alpha}B^3A_1^*\sum_{j=1}^{n}\phi_{yj}\,\phi_{\alpha j}\,\Delta L_j \tag{13}$$

$$D_4 = \frac{\rho}{M_\alpha}B^4A_2^*\sum_{j=1}^{n}\phi_{\alpha j}^2\,\Delta L_j \tag{14}$$

$$E_1 = \frac{\rho}{M_y}B^3H_3^*\sum_{j=1}^{n}\phi_{yj}\,\phi_{\alpha j}\,\Delta L_j \tag{15}$$

$$E_2 = \frac{\rho}{M_\alpha}B^4A_3^*\sum_{j=1}^{n}\phi_{\alpha j}^2\,\Delta L_j \tag{16}$$

Since the torsional damping and stiffness of each TMD are provided by the corresponding properties in vertical direction, the equivalent torsional frequency and damping can be expressed in the forms relating to the vertical properties as follows:

$$\omega_{T\alpha}^{i}=\omega_{Ty}^{i}\, d\sqrt{\frac{m_{Ty}^{i}}{m_{T\alpha}^{i}}} \tag{17}$$

$$\xi_{T\alpha}^{i}=\xi_{Ty}^{i}\,\omega_{T\alpha}^{i}/\omega_{Ty}^{i} \tag{18}$$

where m_{Ty}^{i} and $m_{T\alpha}^{i}$ are the vertical mass and torsional mass inertia of the *i*th TMD, respectively.

To control both the vertical and the torsional response effectively, the frequencies of the central TMD should be tuned around the frequencies of the first vertical and torsional modes of the structure. After selecting these frequencies, the frequency bandwidth, which is the most important parameter in the design, is determined. In this study, this frequency bandwidth is defined as the difference between the maximum and the minimum frequencies of the dampers divided by the effective frequency of the bridge at the design wind speed. If the vertical mass ratio of *i*th damper is determined, one can obtain the vertical mass, and then evaluate the torsional mass inertia by using Eq. (17). The equivalent damping is easily calculated with Eq. (18).

Using the complex forms of the generalized displacements and the external forces in Eqs. (7)~(10), one can obtain

$$\mathbf{G}(\omega)\,\mathbf{A}=\mathbf{F} \tag{19}$$

where **G** is a square matrix of the rank 2N+2; **A** is the amplitude matrix; **F** is the force matrix.

Then, the transfer function can be stated as

$$\mathbf{H}(\omega)=\mathbf{G}^{-1}(\omega) \tag{20}$$

2.1. Buffeting response

As the buffeting response is considered, the buffeting forces acting on deck node *j* in vertical direction L_{bj} and in torsional direction Mo_{bj} are well-known as (Simiu and Scanlan 1986).

$$L_{bj}=\frac{1}{2}\rho U^{2}B\left[C_{L}\frac{2u}{U}+\left(\frac{dC_{L}}{d\alpha}+C_{D}\right)\frac{w}{U}\right]\Delta L_{j} \tag{21}$$

$$Mo_{bj}=\frac{1}{2}\rho U^{2}B^{2}\left[C_{M}\frac{2u}{U}+\frac{dC_{M}}{d\alpha}\frac{w}{U}\right]\Delta L_{j} \tag{22}$$

where C_L, C_D and C_M are the lift, drag and moment coefficients, respectively; u, w are the wind speed fluctuations in horizontal and vertical directions, respectively. The spectra and cross-spectra of horizontal and vertical wind speed fluctuations used in this study are stated as follows (Simiu and Scanlan 1986):

For the spectrum of horizontal wind speed fluctuations

$$S_{u}(n)=\frac{200\dfrac{z}{U}u_{*}^{2}}{\left(1+50\dfrac{nz}{U}\right)^{5/3}} \tag{23}$$

For the spectrum of vertical wind speed fluctuations

$$S_w(n) = \frac{3.36\frac{z}{U}u_*^2}{1+10\left(\frac{nz}{U}\right)^{5/3}} \tag{24}$$

For the cross-spectrum of horizontal and vertical wind speed fluctuations

$$S^C_{r_i r_j}(n) = S_r(n)\exp\left[-\frac{C_r n\,|x_i - x_j|}{U}\right];\ (r = u,\ w) \tag{25}$$

where n is frequency; u_* is the friction velocity; z is the height above ground; C_r is the empirical constants, 16 and 8 are used for the horizontal and vertical wind speed fluctuations, respectively; x_i and x_j are the longitudinal coordinates of nodes i and j, respectively.

The buffeting force spectrum can be obtained by using Eqs. (21)~(25) and the admittance function X^2_{aero}, which is given by (Liepmann 1952).

$$X^2_{aero} = \frac{1}{1+2\pi^2\left(\frac{nB}{U}\right)} \tag{26}$$

Using the random theory and the generalized force spectrum $\mathbf{S_F}$, we can obtain the generalized displacement spectrum $\mathbf{S_R}$

$$\mathbf{S_R} = \mathbf{H}(\omega)\,\mathbf{S_F}\mathbf{H}^*(\omega)^T \tag{27}$$

in which $\mathbf{H}^*(\omega)$ is the conjugate of $\mathbf{H}(\omega)$. Integrating Eq. (27) with the frequency ω, we can obtain the mean square of the generalized displacement σ_s^2

$$\sigma_s^2 = \int_0^\infty \mathbf{S_R}\,d\omega \tag{28}$$

The variance of the displacement in natural coordinate can be easily obtained by using the modal matrix and Eq. (28). It should be noted that the response calculation is based on the first vertical and the first torsional structural modes, and only these modes are taken into account for the analysis.

2.2. Flutter

The use of TMD can not only reduce the buffeting response, it can increase the critical velocity. The common types of flutter on long-span bridges are single-degree-of-freedom flutter and coupled mode flutter. The latter results from the involvement of the vertical and torsional modes that should be included in the formulations to precisely predict the critical velocity of the bridge. In this proposed model, both the vertical and torsional modes are used and the aerodynamic coupling between modes is considered. Therefore, it is capable of raising the critical velocity for either type of flutter.

Since the external force is not relevant with the flutter analysis, the external force term in

Eq. (19) is dropped. With some rearrangements, a complex eigen-value problem is yielded and can be stated in a matrix form

$$(\mathbf{S}-\mathbf{D})\mathbf{A}=0 \tag{29}$$

where $\mathbf{D}$ is a diagonal matrix = Diag[ω^2]; $\mathbf{A}$ is an amplitude matrix; $\mathbf{S}$ is a square matrix = $\mathbf{G}+\mathbf{D}$.

It is noted that Eq. (29) should be solved by iteration for each wind speed, because the matrix $\mathbf{S}$ contains the unknown ω. The flutter is identified as the imaginary part of ω is equal to zero. Meanwhile, the corresponding wind speed is recognized as the critical velocity. The iterative calculation can yield a convergent solution by using an appropriate initial value and a reliable convergence criterion.

3. Examples

There are two examples presented to demonstrate the performance of the proposed MTMDs. Example 1 is a cable-stayed bridge with a set of flutter derivatives in which the aerodynamic coupling is significant. Example 2 is also a cable-stayed bridge but with a different set of flutter derivatives in which aerodynamic coupling is not significant. The structures used in these examples have the same geometry but different sectional properties. The bridges have a total span of 1460 m and a width of 28 m for Example 1 and 21.5 m for Example 2. Two 200-m-high towers are supported by cables. The geometry of the bridges is shown in Fig. 3. A finite element model, consisted of beam elements and cable elements, is used to calculate the natural frequencies of the structure. Through the calculation, the natural frequencies of the first vertical mode and the first torsion mode are 0.143 Hz and 0.2856 Hz, respectively for Example 1, and 0.143 Hz and 0.354 Hz, respectively for Example 2. The two sets of flutter derivatives H_i^* and A_i^* (i = 1, 2, 3), adopted from Scanlan and Tomko (1971), are shown in Fig. 4. The lift and torsion coefficients C_L and C_M, used for buffeting calculations, are adopted from wind tunnel investigations of the Kao Ping Hsi bridge (1994) and shown in Fig. 5. The structural damping is 1% and the air density is 1.22 kg/m^3. To simplify the analysis, several assumptions are made here. First, the frequency interval of the MTMDs is the same. Second, the mass and the damping of each damper are also the same. Third, the dampers are connected to the bridge at the middle point of the center span where the maximum response will occur.

3.1. Example 1

Due to the aerodynamic damping, the effective damping of the bridge will be altered. The

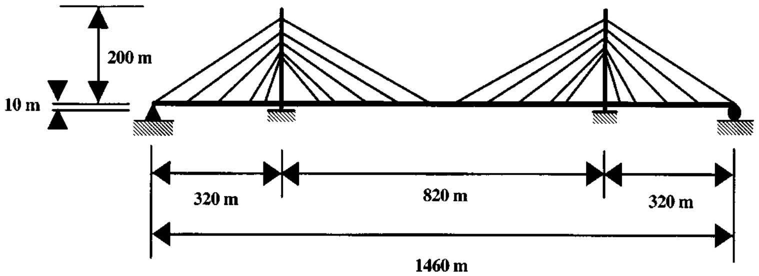

Fig. 3 Geometry of the cable-stayed bridge

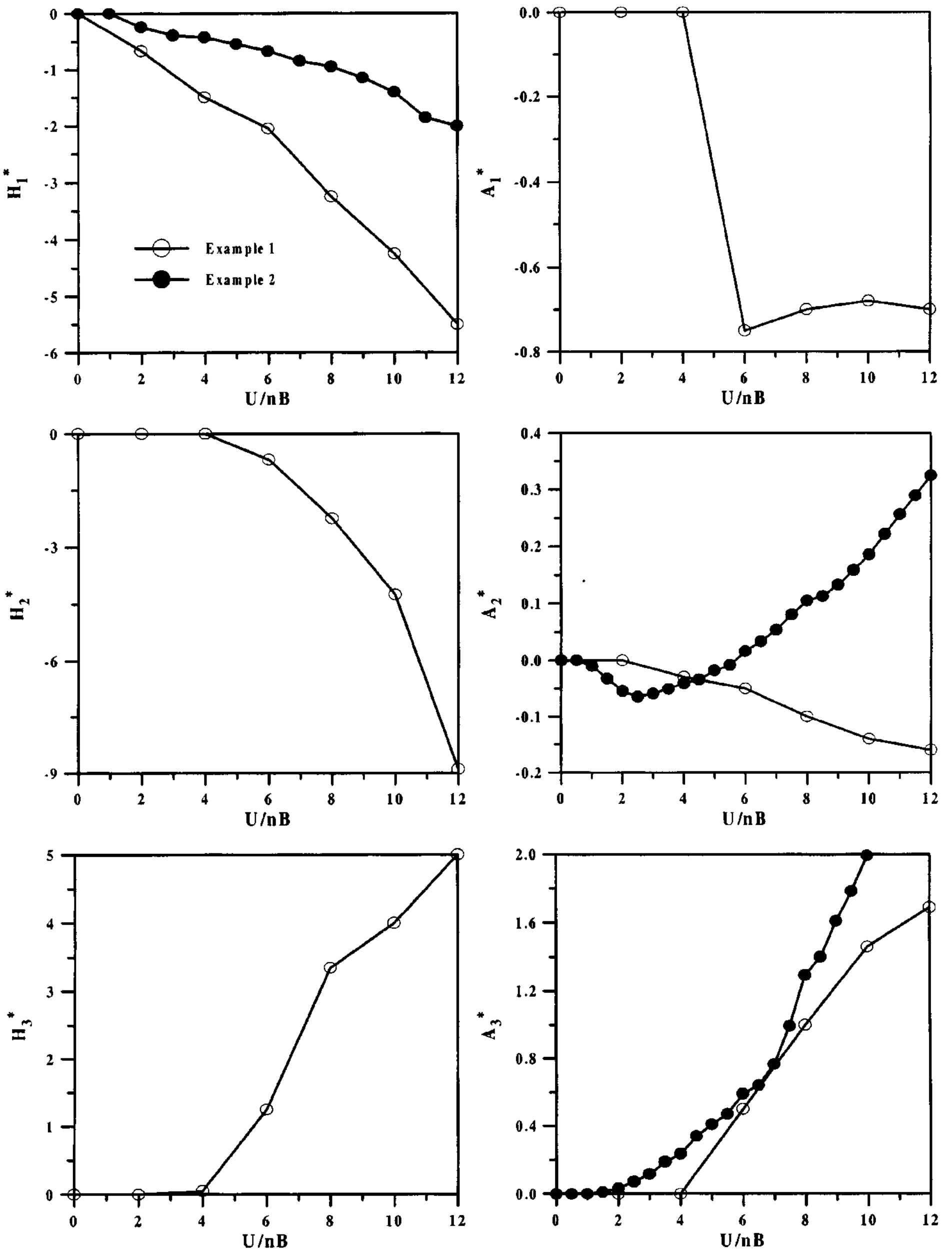

Fig. 4 Flutter derivatives

vertical and torsional damping of the bridge without using the MTMDs versus mean wind speed are shown in Figs. 6-7, respectively. To examine the performance of the proposed model, the MTMDs, designed with total vertical mass ratio $\mu_y = 2\%$, total torsional mass ratio $\mu_\alpha = 0.716\%$, vertical damping ratio $\xi_{Ty} = 1.5\%$, torsional damping ratio $\xi_{T\alpha} = 2.6\%$, number of TMDs N = 9, frequency bandwidth B = 0.2, central TMD's vertical frequency $n_{Ty} = 0.143$ Hz and torsional frequency $n_{T\alpha} = 0.252$ Hz, are used in this analysis. The buffeting response reductions

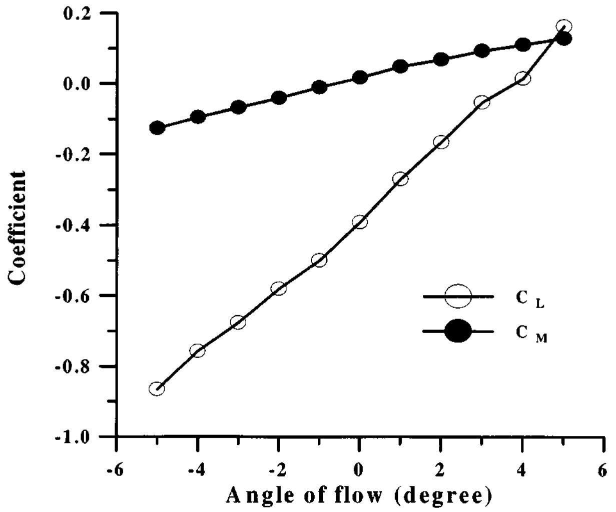

Fig. 5 Lift and torsional coefficients

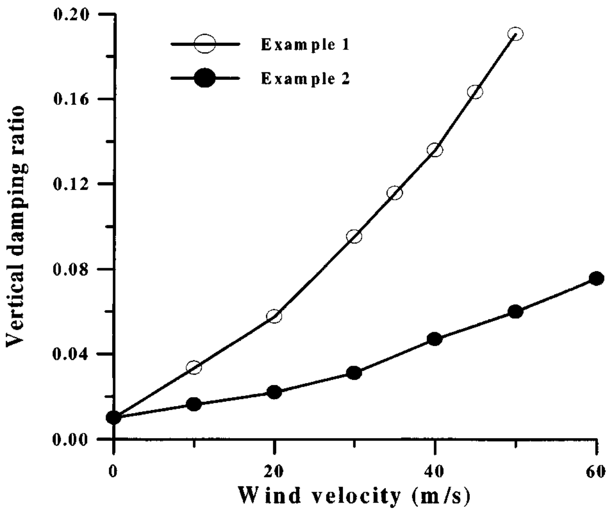

Fig. 6 Vertical damping ratio versus wind speed

of the bridge with using the MTMDs in vertical and torsional directions versus wind speed are shown in Fig. 8. For comparison, the performance of the optimized single TMD (with 2 DOF) is also shown in this figure. The results show that the proposed MTMDs do not only effectively suppress buffeting in both directions, but are more effective than the single TMD. The critical velocity of the bridge is increased by the MTMDs from 53.55 m/s to 65.72 m/s, compared to the single TMD's, 64.56 m/s. It should be noted that the aerodynamic coupling is significant in this bridge and this effect should be incorporated into the formulations to calculate the response precisely. The influence of the aerodynamic coupling on torsional response can be clearly identified in Fig. 9.

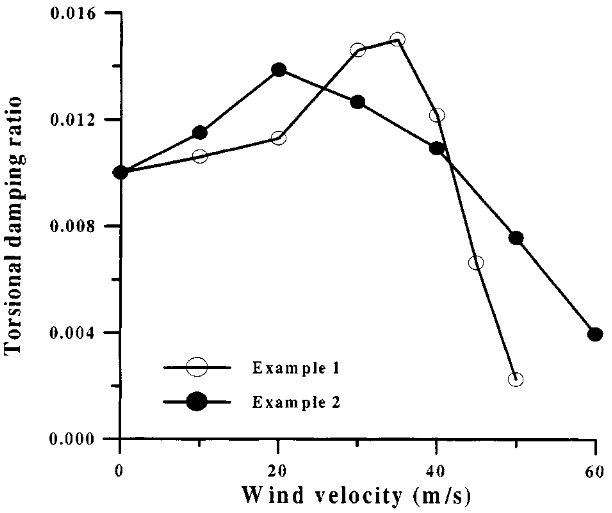

Fig. 7 Torsional damping ratio versus wind speed

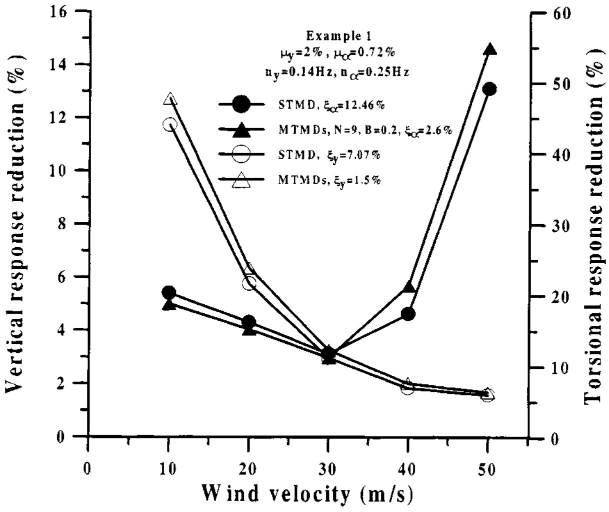

Fig. 8 Performance versus wind speed of the proposed MTMDs (example 1)

3.2. Example 2

The vertical and torsional damping of the bridge without using the MTMDs versus mean wind speed are also shown in Figs. 6~7, respectively. The vertical mass ratio and vertical damping ratio of the MTMDs used in this bridge are the same as those in Example 1, but the equivalent torsional mass ratio and damping ratio are 0.424% and 3.2% and the vertical and torsional frequencies of the central TMD are 0.143 Hz and 0.328 Hz, respectively. The buffeting response reductions of the bridge with using the MTMDs in vertical and torsional directions versus wind speed are shown in Fig. 10. The results indicate that the proposed dampers are effective for suppressing both the vertical and torsional responses and superior to

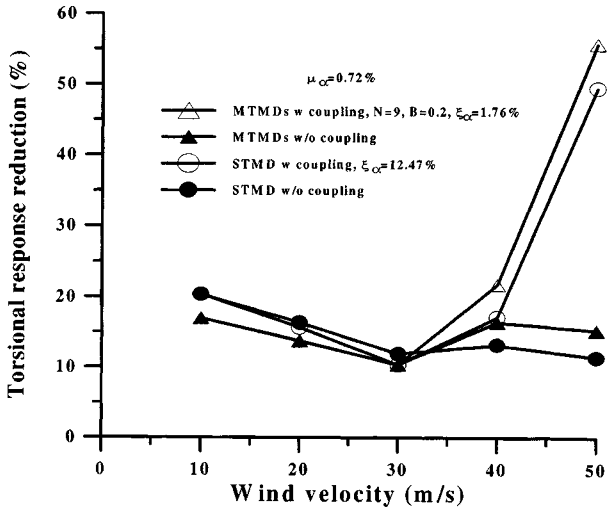

Fig. 9 Comparisons of torsional performance between a single TMD and MTMDs

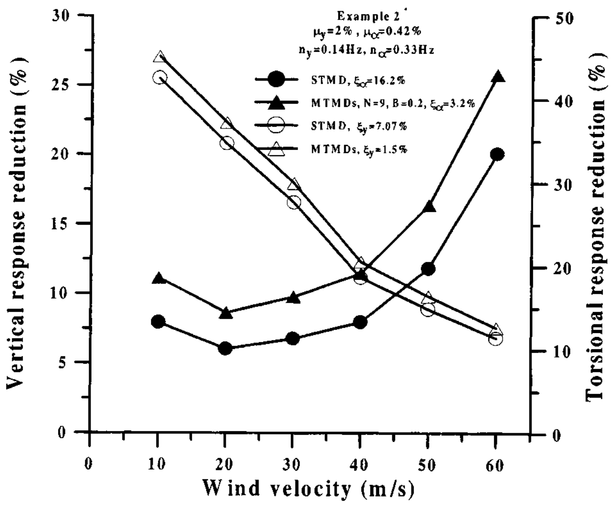

Fig. 10 Performance versus wind speed of the proposed MTMDs (example 2)

the single TMD. The critical velocity of the bridge without using TMD is 68.3 m/s. This critical velocity can be increased to 75.42 m/s by using the single TMD, and 88.7 m/s by using the proposed MTMDs.

4. Effects of the MTMDs parameters on response

A parametric study, based on the bridge used in Example 1, is presented to investigate the effects of the design parameters of the MTMDs. In this model, the torsional mass ratio and the torsional damping ratio are dependent on the corresponding properties in the vertical direction. Therefore, the design parameters to be studied only include the total vertical mass ratio, the vertical damping ratio, the number of dampers, the frequencies of the central damper and the frequency bandwidth. To account for the mistuning problem, offset effect is also considered. From Figs. 6~7, it can be seen that the vertical damping of the bridge in Example 1 increases with wind speed but the torsional damping decreases. Consequently, the performance of the MTMDs decreases with the wind velocity on vertical response but increases with wind velocity on torsional response. Hence, the following parameters are studied at the wind speed 10m/s for vertical response and 50m/s for torsional response only.

4.1. Effects of damping ratio

When 2% total mass ratio is used, the relationships between the response reduction ratio and the damping ratio for various frequency bandwidths in both vertical and torsional directions are shown in Figs. 11~12, respectively. From these figures it is seen that the optimum damping ratio of the MTMDs is smaller than that of a single TMD. In addition, the MTMDs are less effective for a higher damping ratio. As we would expect, these characteristics of the MTMDs are the same as those in previous studies. The results in Fig. 11 also show that the vertical frequency range 0.2 yields the best performance for any number of TMDs and the corresponding optimum damping ratio is approximately 2%, except in the case of 3 TMDs. The results in Fig. 12 indicate that the maximum torsional performance occurs with the frequency range 0.1 for each case and

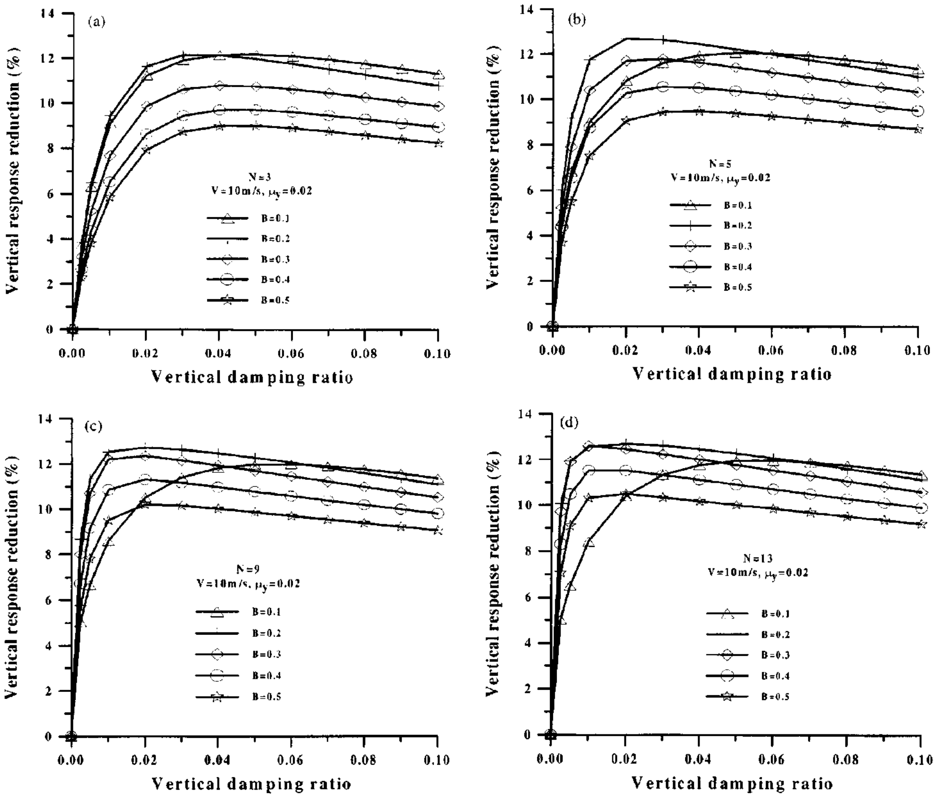

Fig. 11 Vertical response reduction ratio versus TMD damping (a; n=3, b; n=5, c; n=9, d; n=13)

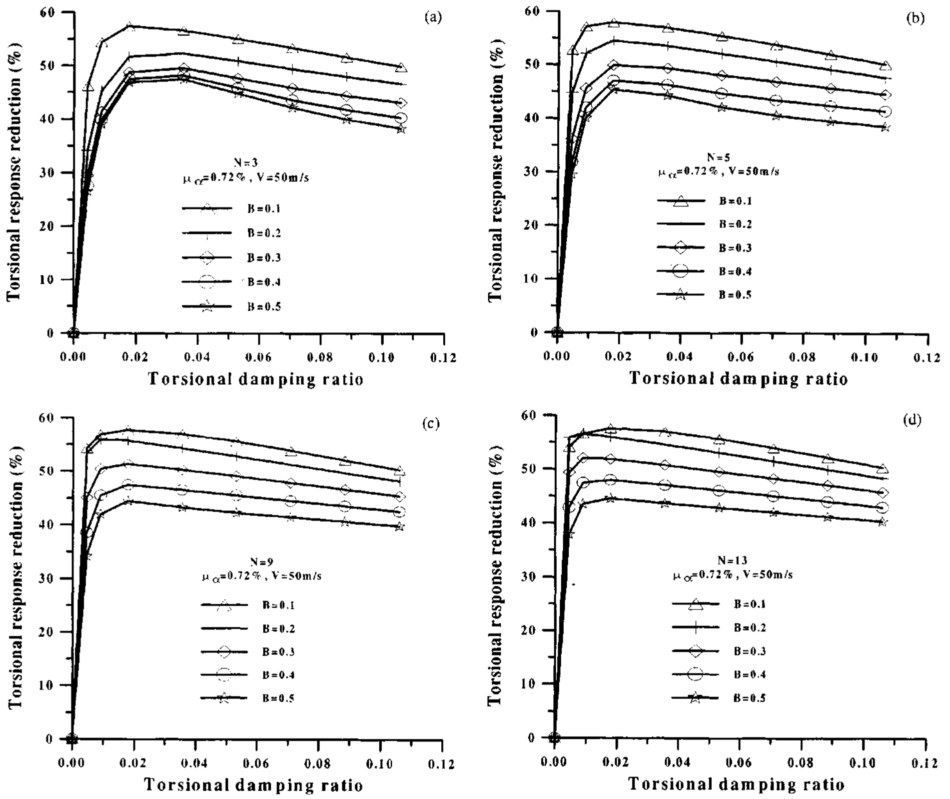

Fig. 12 Torsional response reduction ratio versus TMD damping (a; n=3, b; n=5, c; n=9, d; n=13)

the corresponding optimum torsional damping ratio is around 1.76%. This value corresponds to 1% vertical damping ratio. The smaller bandwidth in torsional direction is due to the smaller torsional mass ratio which is 0.716% compared to the vertical mass ratio 2%. These results reveal that the optimum values of frequency bandwidths and damping ratios in vertical and torsional directions are not consistent. Since the torsional frequency is dependent upon the vertical frequency, the vertical and torsional frequency bandwidths should be the same. Also, the optimum damping ratios in both directions will not occur simultaneously, because the torsional damping is related to the vertical damping. To ensure the performance of the MTMDs in both vertical and torsional directions, we can suggest that 1%~2% vertical damping is appropriate for the MTMDs with 2% total mass ratio. In this damping range, the higher value is better suited for the smaller number of TMDs.

4.2. Effects of bandwidth

The bandwidth is one of the most important design parameters of the MTMDs. It designates the range of the distributed frequencies of the TMDs and is defined here as the ratio of the difference between the maximum and the minimum frequencies of the TMDs to the effective structural frequency. Fig. 13 shows the response reduction ratio versus bandwidth for different numbers of TMDs. It can be seen from Fig. 13a that the optimum bandwidth increases

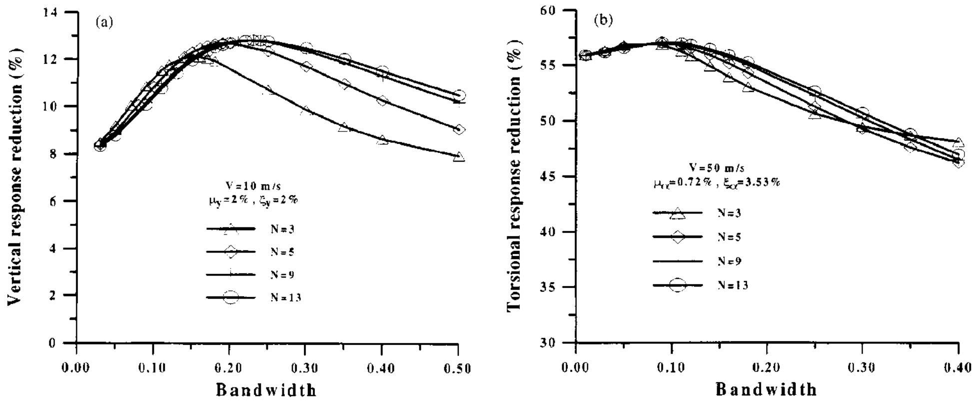

Fig. 13 Performance versus bandwidth for different number of dampers (a) vertical response (b) torsional response

with the number of TMDs and tends to converge to a value of about 0.2 as the number is equal to or larger than 9. In torsional direction, Fig. 13b indicates that the optimum bandwidth is around 0.1 for any number of TMDs. These inconsistent results in both directions were stated earlier. The sharp decrease of vertical response reduction ratio can be clearly seen when the bandwidth is less than 0.2. On the other hand, the decrease of torsional performance is not so obvious when the bandwidth is larger than 0.1. Therefore, it can be concluded that the effects of the bandwidth are more significant for vertical performance than for torsional performance. In practice, the design engineer first determines which direction of vibration is more important, and then selects an appropriate value between 0.1 and 0.2, or just simply chooses 0.2 because of the less sensitive torsional performance.

4.3. Effects of the number of TMDs

From Figs. 12~13, it is seen that the performance increases with the number of TMDs and achieves the maximum as the number is 9. Although the differences of performance between various numbers of TMDs are not so significant, the number of TMDs should be large enough to maintain the advantages of the MTMDs. Conversely, the number of TMDs should be limited, because too many dampers might induce the difficulties to tune the frequencies precisely. For the above reasons, the suggested number is approximately 9.

4.4. Effects of mass ratio

It is known that the performance of the MTMDs increases with the mass ratio and the optimum damping ratio also increases. To study this effect, we use 9 TMDs and bandwidth of 0.15 for the analysis. The relationship between the response reduction ratio and the damping ratio for different mass ratios is shown in Fig. 14. The results indicate that the increase of vertical response reduction ratio is more significant when the mass ratio is raised from 1% to 2% than 2% to 3%. The similar trend is also seen in torsional direction. For design purpose, the appropriate value of total mass ratio is about 2%.

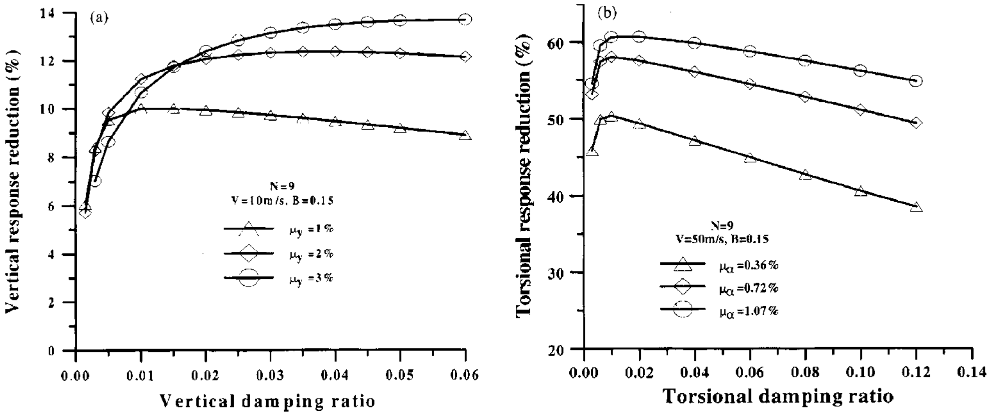

Fig. 14 The effects of mass ratio on response reduction ratio (a) vertical response (b) torsional response

4.5. Robustness

The natural frequency discrepancies between the real structure and the prototype are, in

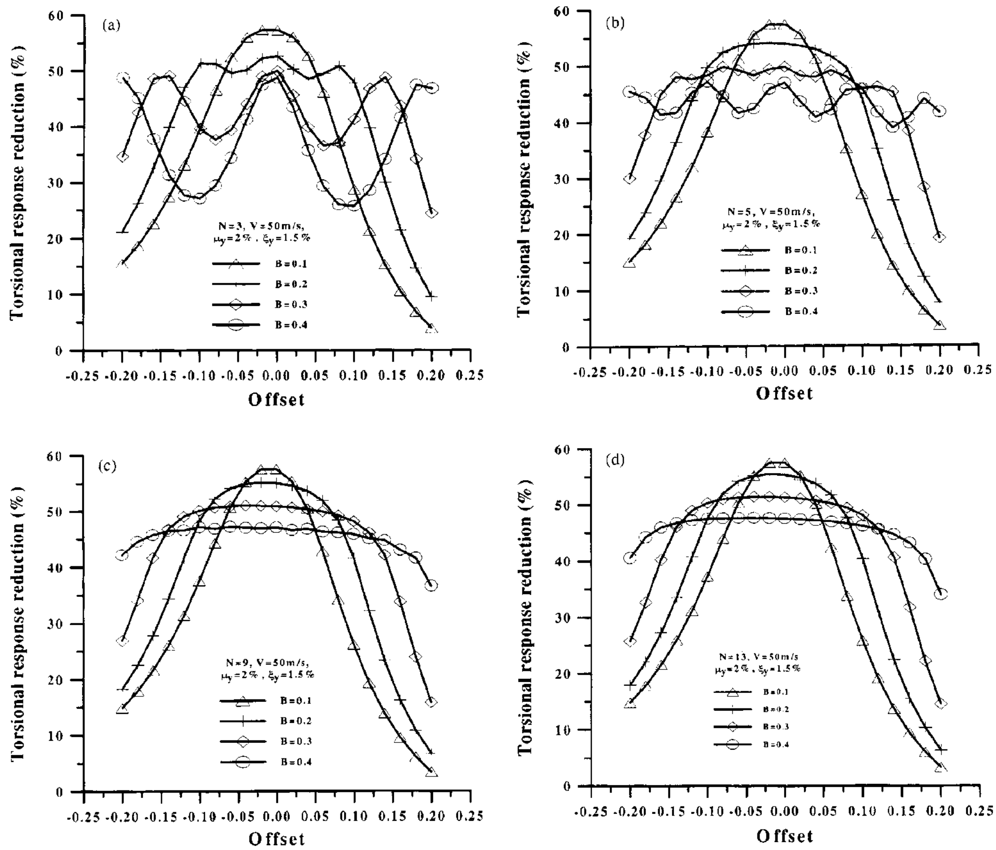

Fig. 15 Torsional response reduction ratio versus frequency offset (a; n=3, b; 5, c; n=9, d; n=13)

Table 1 Increase of the critical velocity of Example 1 and 2

Number of dampers	Total vertical damping(%)	Frequency bandwidth	Critical velocity(m/s)	
			Example 1	Example 2
1	7.07	-	64.56	75.42
9	1.5	0.1	62.18	77.73
9	1.5	0.2	65.72	88.68

practice, inevitable. In addition, the effective torsional frequency of the bridge is affected by the aeroelastic stiffness. For these reasons the offset problems should be taken into account for determining the design parameters to guarantee the minimum performance. Because the total number of TMDs and bandwidth will affect the robustness, these factors are studied in the following analysis.

At 50 m/s wind speed, the torsional response reduction ratio against offset for 3, 5, 9 and 13 TMDs are plotted in Fig. 15. In these figures, the total vertical mass ratio is 2% and the vertical damping ratio is 1.5%. From these results, it is seen that the robustness increases with the bandwidth but the performance decreases. To satisfy both robustness and performance requirements, a bandwidth of 0.2 appears to be a best value for any number of TMDs. This value is also suggested in earlier sections. It is also seen that, for a given bandwidth, more TMDs are more robust and produce better performance. Therefore, 9 or 13 TMDs are better than 3 and 5 TMDs. However, the comparison of the results between 9 and 13 TMDs indicates that the performance of 13 TMDs is almost the same as that of 9 TMDs. The conclusion can be drawn, suggested earlier, that the best number of TMDs is approximately 9.

4.6. Increase of critical velocity

Without using dampers, the critical velocities of the bridges in Example 1 and 2 are 53.55 and 68.33 m/s, respectively. The types of flutter in Example 1 and 2 designate coupled flutter and single-degree-of-freedom flutter, respectively. An optimized single TMD and 9 TMDs with different bandwidths are analyzed to study the increase of the critical velocity by the addition of the tuned mass dampers. The total generalized mass ratio of 2% is used. With the addition of the MTMDs to the bridge, the maximum increase of the cable tension is less than 1%. The frequency of the dampers is taken as the effective frequency at the design wind speed, although this frequency can be tuned less for achieving the maximum stability. The results of Example 1 and 2, illustrated in Table 1, indicate that the critical velocity of the bridge with using TMDs is 16~23% higher than that of the bridge without using TMDs in the case of coupled flutter and 10-30% higher in the case of single-degree-of-freedom flutter. It is also found that the bandwidth 0.2 is better than 0.1 for the 9 dampers. Comparison of a single TMD and the MTMDs indicates that the MTMDs are more effective for increasing the structure's stability.

5. Design procedures of the proposed MTMDs

From the results discussed above, the design procedures of the proposed MTMDs can be summarized as follows:

1. Choose the frequencies of the central TMD. One can just simply take the natural frequency of the first vertical mode and the effective frequency of the first torsional mode at the design wind speed as the ones of the central TMD. If the bridge's stability is the major concern, then choose the flutter frequency of the bridge, without using the TMD, as the frequency in torsional direction.
2. Choose the number of dampers and determine the frequency bandwidth. The suggested number is approximately 9, and the bandwidth is 0.2.
3. Select the total vertical mass ratio and evaluate its corresponding damping ratio. To ensure the performance in vertical direction, the total vertical mass ratio is suggested to be 2% and the corresponding damping ratio is 2%.
4. Calculate the equivalent torsional mass ratio and damping ratio by using Eqs. (17)~(18).

6. Conclusions

The MTMDs are proposed for suppressing both the vertical and the torsional buffeting responses and for increasing the structural stability of long-span bridges. A parametric analysis is performed to examine the validity and applicability of the proposed MTMDs. Through this analysis, the suggested design parameters including damping, mass, number, and bandwidth of the MTMDs are recommended and the design procedures are provided. Based on these results, the following conclusions are made:

1. The proposed MTMDs not only maintain the characteristics of the conventional MTMDs but also have the capability of controlling vertical and torsional responses simultaneously. In example 1, the case with significant aerodynamic coupling, the maximum vertical and torsional responses are reduced by 13% and 55%, respectively. In example 2, the case with minor aerodynamic coupling, the maximum vertical and torsional responses are reduced by 27% and 43%, respectively. In addition, these MTMDs are slightly more effective than an optimized single TMD.
2. The MTMDs are able to increase the critical speed of a bridge for either single-degree-of-freedom flutter or coupled flutter. The critical speed is increased by 23% in example 1 and increased by 30% in example 2. For increasing the aerodynamic stability of a bridge, the MTMDs are also more effective than an optimized single TMD.
3. For effectively suppressing the buffeting responses and increasing the critical speed, the suggested tuning frequencies of the central damper are the effective frequencies of the first flexural and torsional modes at the design wind speed.
4. The suggested number of dampers is 9 or more, and the corresponding frequency bandwidth is 0.2.
5. The total vertical mass is suggested to be 2% or more to ensure the vertical performance, and the corresponding damping ratio is 2%. The torsional mass and damping in this model are dependent on those in vertical direction, these parameters can be calculated after the vertical properties have been determined.

Acknowledgements

The writers gratefully acknowledge the financial support of part of this work by the

National Science Council (R. O. C.) under the grant NSC 87-2211-E-032-017.

References

Abe, M. and Fujino, Y. (1994), "Dynamic characterization of multiple tuned mass dampers and some design formulas", *Earthquake Eng. Struct. Dyn.*, **23**, 813-835.

Abe, M. and Igusa, T. (1995), "Tuned mass dampers for structures with closely spaced natural frequencies", *Earthquake Eng. Struct. Dyn.*, **24**, 247-261.

Gu, M., Chang, C.C., Wu, W. and Xiang, H.F. (1998), "Increase of critical flutter wind speed of long-span bridges using tuned mass dampers", *J. Wind Eng. Ind. Aerodyn.*, **73**, 111-123.

Honda, A. *et al.* (1993), "Aerodynamic stability of Kansai international airport access bridge", *J. Wind Eng. Ind. Aerodyn.*, **49**, 533-542.

Huffmann, G., Freeman, R.A. and Brown, C.W. (1987), "Dao Khanong cable stayed bridge: tuned mass dampers in deck and pylon", *Proc. int. Conf. on Cable Stayed Bridges*, Bangkok, 1485-1493.

Igusa, T. and Xu, K. (1994), "Vibration control using multiple tuned mass dampers", *J. Sound Vib.*, **175**(4), 491-503.

Jangid, R.S. and Datta, T.K. (1997), "Performance of multiple tuned mass dampers for torsionally coupled system", *Earthquake Eng. Struct. Dyn.*, **26**, 307-317.

Kareem, A. and Kline, S. (1995), "Performance of multiple mass dampers under random loading", *J. Struct. Eng., ASCE*, **121**, 348-361.

Liepmann, H.W. (1952), "On the application of statistical concepts to the buffeting problem", *J. Aero. Sci.*, **19**(12), 793-800.

Lin, Y.Y., Cheng, C.M. and Lee, C.H. (1999), "A tuned mass damper for suppressing the coupled flexural and torsional buffeting response of long-span bridges", *Eng. Struct.*(paper accepted)

Malhortra, P.K. and Wieland, M. (1987), "Tuned mass damper for suppressing wind effects in a cable-stayed bridge", *Proc. int. Conf. on Cable Stayed Bridges*, Bangkok, 557-568.

Nobuto, J., Fujino, Y. and Ito, M. (1988), "A study on the effectiveness of TMD to suppress a coupled flutter of bridge deck", *Proc. JSCE*, No. 398/I-10, 413-416.

Scanlan, R.H. and Tomko, J.J. (1971), "Airfoil and bridge deck flutter derivatives", *J. Eng. Mech. Div., ASCE*, **97**, 1717-1737.

Simiu, E. and Scanlan, R.H. (1986), *Wind Effects on Structures*, 2nd ed., John Wiley & Sons, New York, N. Y.

Sun, D. (1997), "Wind-induced vibration control of long-span bridges by multiple tuned mass dampers", MS thesis, Civ. Eng. Dept., Tamkang Univ., Taiwan. (in Chinese)

Xu, K. and Igusa, T. (1992), "Dynamic characteristics of multiple substructures with closely spaced frequencies", *Earthquake Eng. Struct. Dyn.*, **21**, 1059-1070.

Yamaguchi, H. and Harnpornchai, N. (1993), "Fundamental characteristics of multiple tuned mass dampers for suppressing harmonically forced oscillations", *Earthquake Eng. Struct. Dyn.*, **22**, 51-62.

Wind tunnel investigations of the Kao Ping Hsi bridge (1994), Taiwan Area National Expressway Engineering Bureau, Taipei, Taiwan, 1994.

(Communicated by Ahsan Kareem)